

Electronic Supporting Information

A self-adaptive film for passive radiative cooling and solar heating regulation

Xue Mei^a, Tong Wang^{b*}, Min Chen^a, Limin Wu^{a*}

Corresponding authors. Email: lmw@fudan.edu.cn (L. W.); wangtong@usst.edu.cn (T. W.)

1. Materials

N-isopropylacrylamine (NIPAm, $\geq 98\%$), N, N'-Methylenebis (acrylamide) (BIS, $\geq 99\%$), polyvinylalcohol (PVA, $\geq 99\%$), 2-Hydroxy-2-methylpropiophenone (HMPP, $\geq 97\%$), were purchased from Aladdin without further purification. Trichloro (1H,1H,2H,2H-perfluorooctyl) silane (PFOTS, $\geq 97\%$) was purchased from Sigma without further purification. The poly (vinylidene fluoride) (PVDF) with different thickness (50, 100, 500, 1000 μm) were purchased from Shenzhen Yuxin Plastic Co. LTD.

2. Calculation of passive radiative cooling power and solar heating power

The parameters in Eq. (1) and Eq. (2) can be calculated with the following equations:^{1,2}

$$P_{rad}(T) = A \int d\Omega \cos\theta \int_0^{\infty} d\lambda I_{BB}(T, \lambda) \varepsilon(\lambda, \theta) \quad (3)$$

$$P_{atm}(T_{amb}) = A \int d\Omega \cos\theta \int_0^{\infty} d\lambda I_{BB}(T_{amb}, \lambda) \varepsilon(\lambda, \theta) \varepsilon_{atm}(\lambda, \theta) \quad (4)$$

$$P_{solar} = A \int_0^{\infty} d\lambda \varepsilon(\lambda, \theta_{solar}) I_{AM1.5}(\lambda) \quad (5)$$

$$P_c = Ah_c(T_{amb} - T) \quad (6)$$

$$P_c = Ah_c(T - T_{amb}) \quad (7)$$

Eq. (6) is used to calculate the cooling power in Eq. (1) and Eq. (7) is used to calculate the heating power in Eq. (2). A is the surface area of the test sample involved in

cooling/heating. Here, $\int d\Omega = 2\pi \int_0^{\pi/2} d\theta$ is the angular integral over a hemisphere, $I_{BB}(T, \lambda)$ is the spectral radiance of a blackbody at temperature T , $\varepsilon(\lambda, \theta)$ is the emissivity of the sample in a particular direction and wavelength, and $\varepsilon_{atm}(\lambda, \theta)$ is the angle-dependent emissivity of the atmosphere. h_c is the embodiment of heat conduction and heat convection effects, called the comprehensive non-radiant heat coefficient, and its value is between 0 and 12 W/m²/K.³

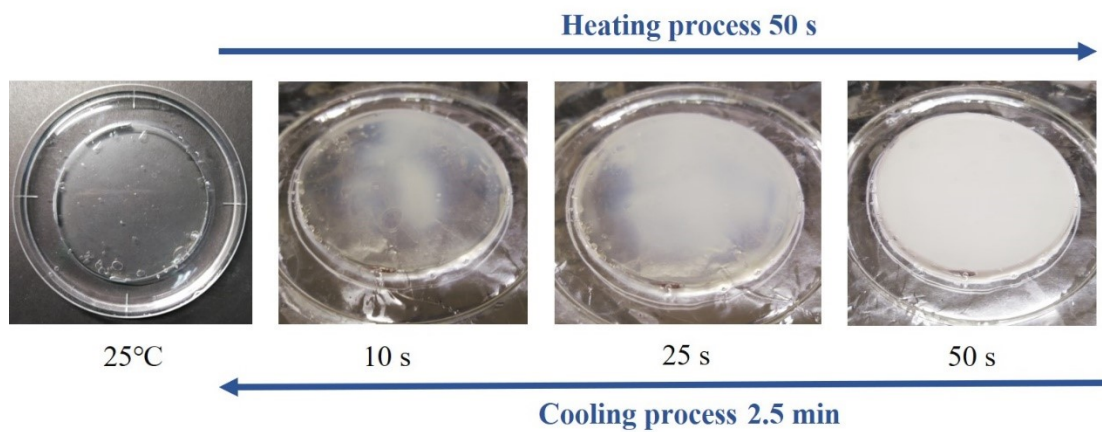


Fig. S1. Response time of PVDF@PNIPAm film during phase change.

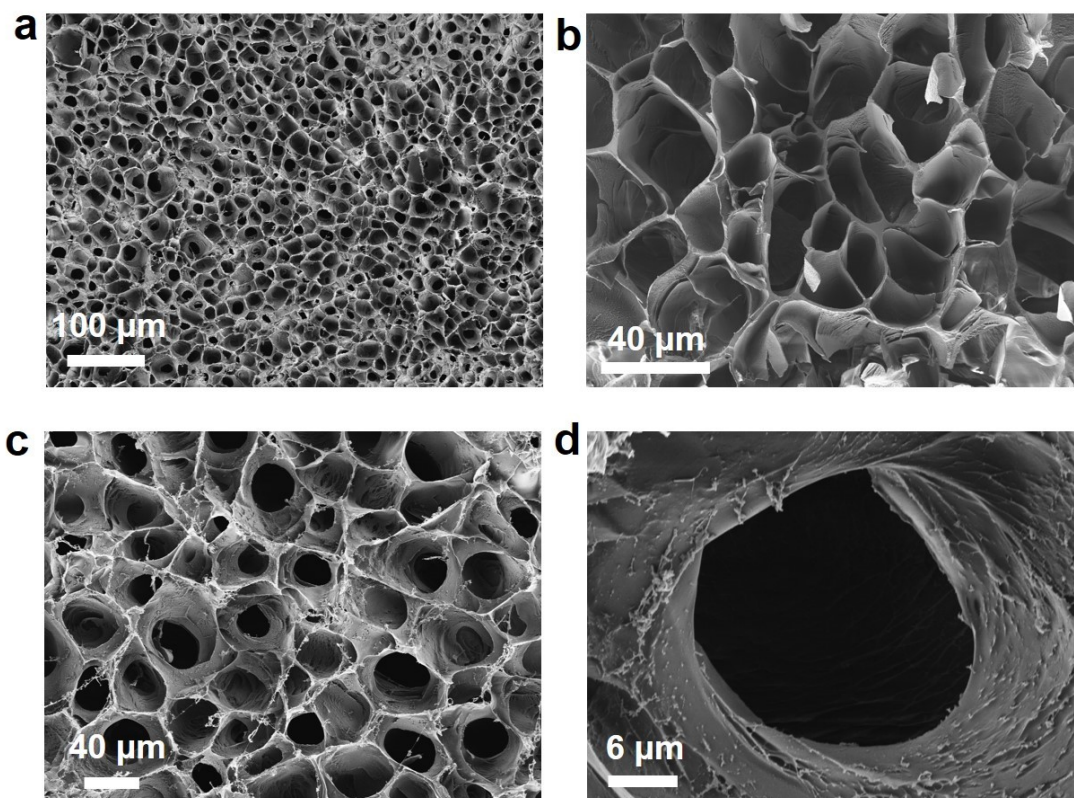


Fig. S2. Scanning electron microscope (SEM) photographs of different sections of PNIPAm hydrogel at different magnifications.

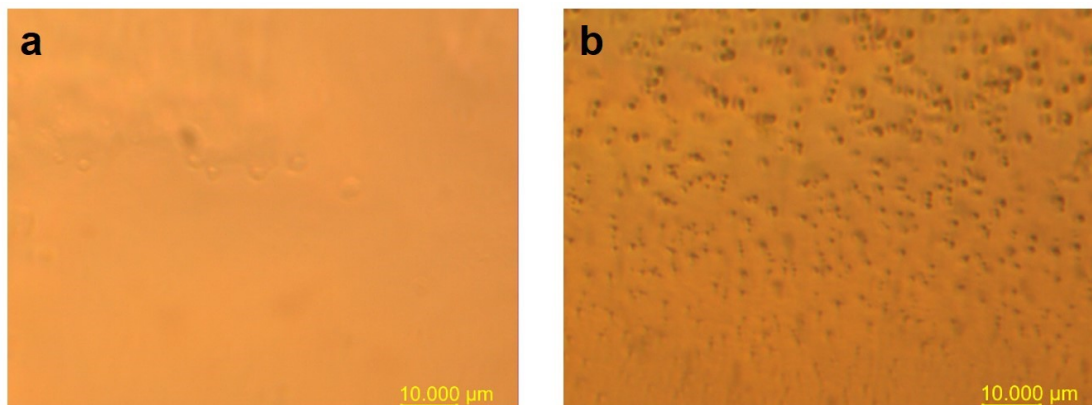


Fig. S3. (a) Optical micrograph of PNIPAm hydrogel at 20 °C. (b) Optical micrograph of PNIPAm hydrogel at 40 °C.

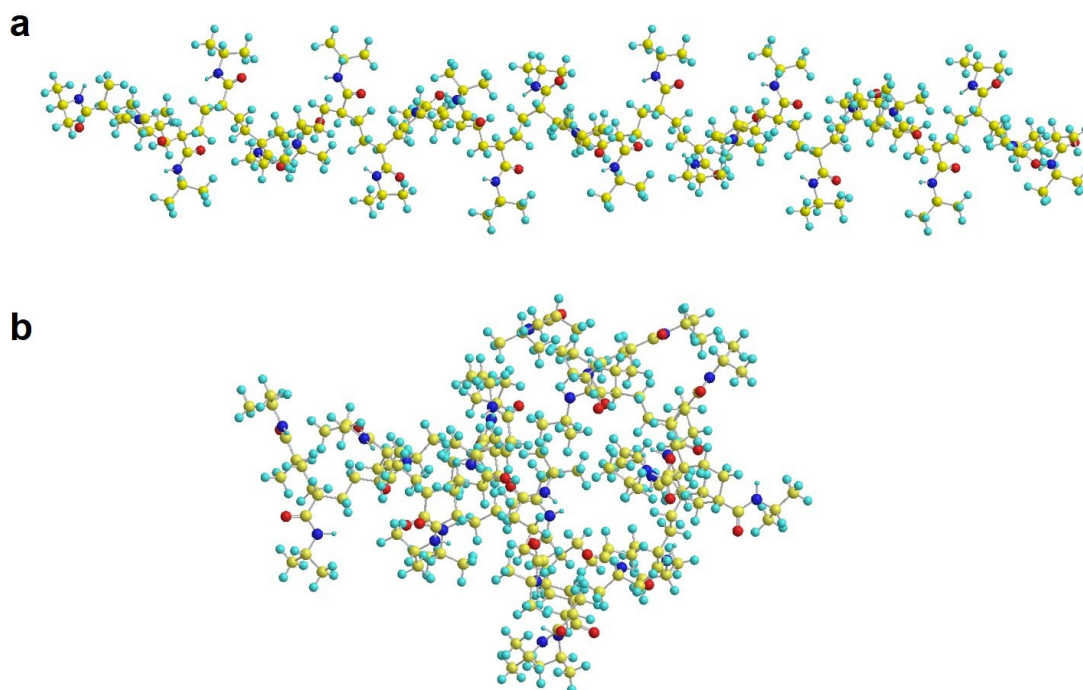


Fig. S4. (a) The relatively stretched PNIPAm molecular chain when the temperature is below LCST. (b) The relatively contracted PNIPAm molecular chain when the temperature is above LCST.

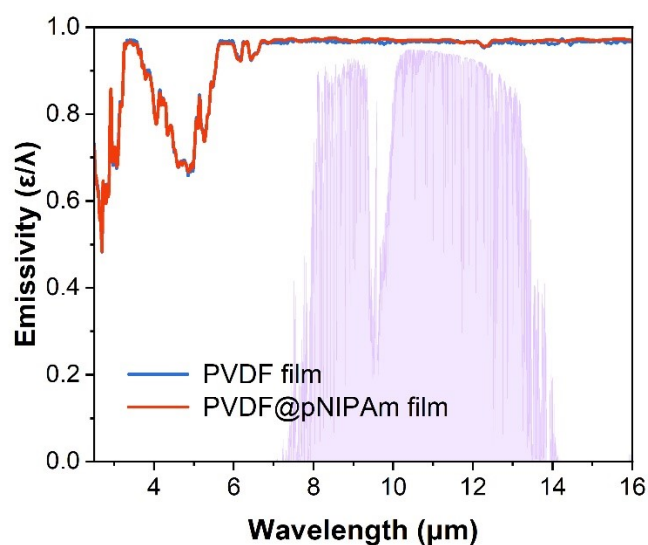


Fig. S5. Longwave infrared (LWIR) emissivity spectra of the PVDF@PNIPAm film and individual PVDF film (1 mm).

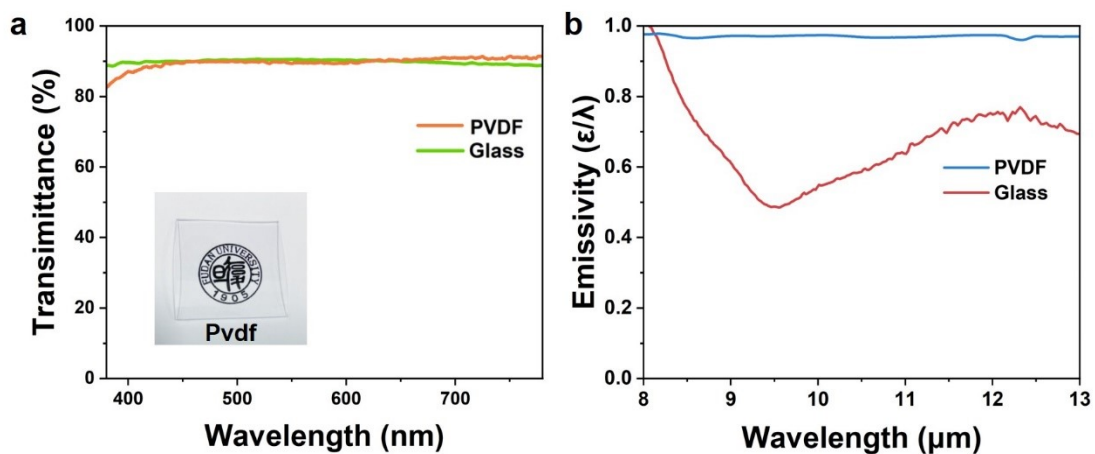


Figure S6. (a) Visible light (380-780 nm) transmittance spectra of individual PVDF film and glass with thickness of 1mm. (b) Longwave infrared (LWIR) emissivity spectra of individual PVDF film and glass with thickness of 1mm.

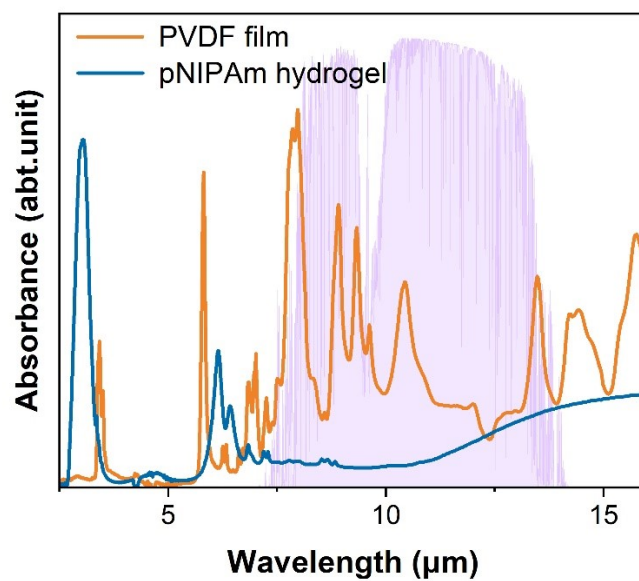


Fig. S7. Comparison of the infrared absorption spectra of the PNIPAm hydrogel and the PVDF film.

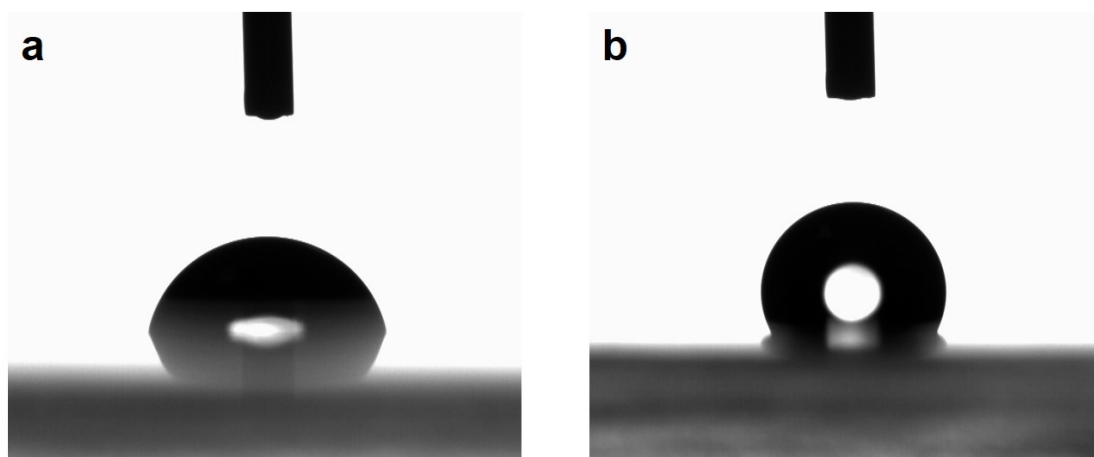


Fig. S8. (a) The water contact angle (WCA) of the untreated PVDF@PNIPAm film. (b) The WCA of the PVDF@PNIPAm film after modified by fluorosilane.

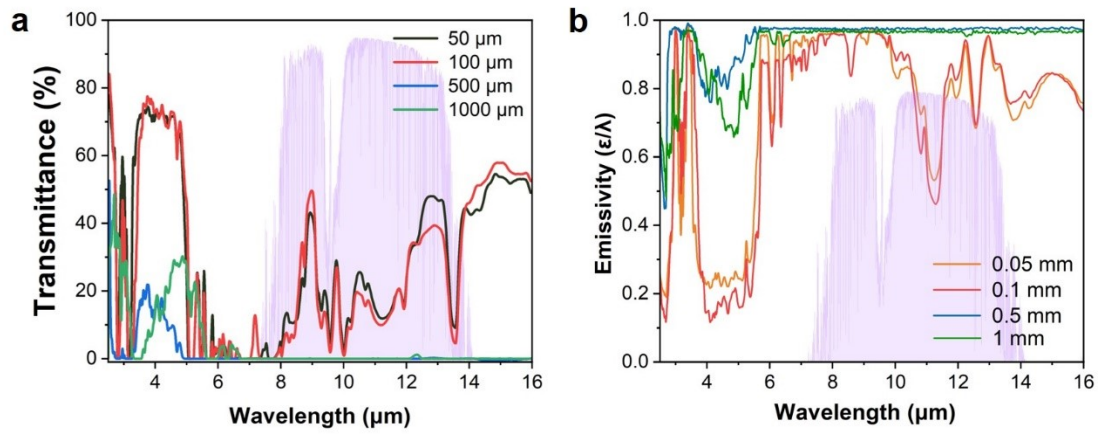


Fig. S9. (a) Variation in infrared transmittance spectra of the PVDF film with different thickness. (b) Variation in infrared emissivity spectra of the PVDF film with different thickness.

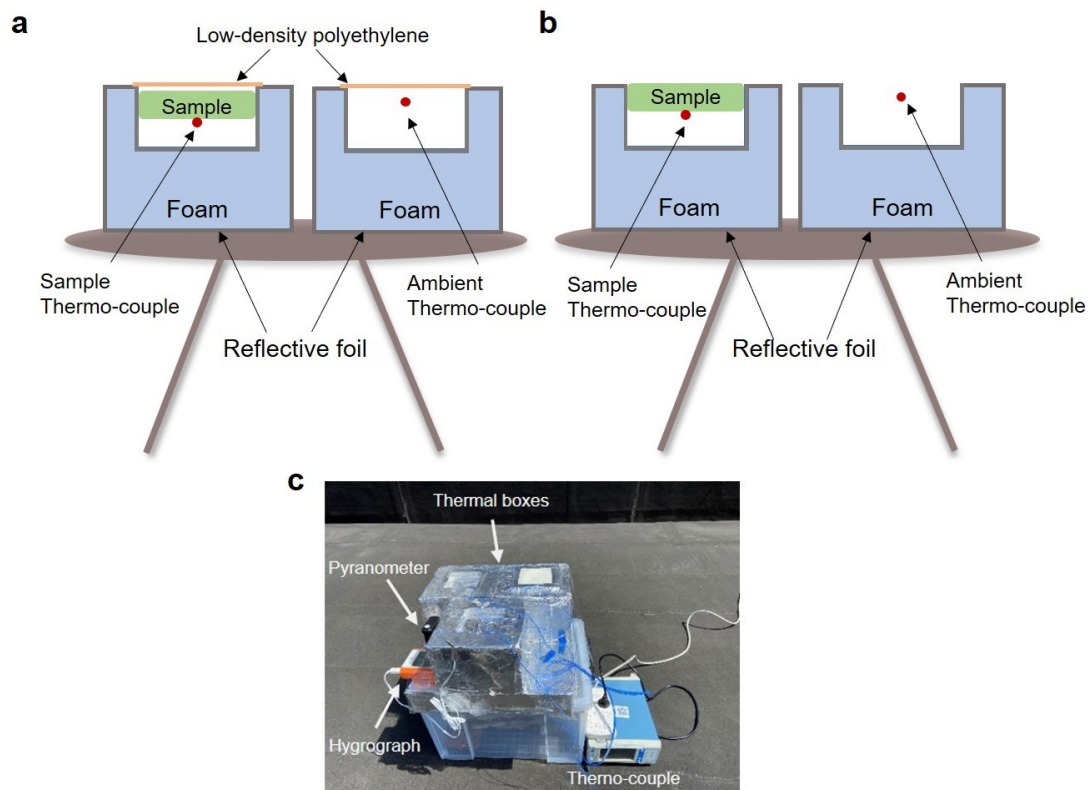


Figure S10. Schematic diagram of different measuring devices: sample surface covered (a) with low-density polyethylene and (b) without LDPE. (c) Photo of the actual measuring device, located on the roof of a fifth floor building, including thermal boxes, a pyranometer, a hygrograph and thermo-couples.

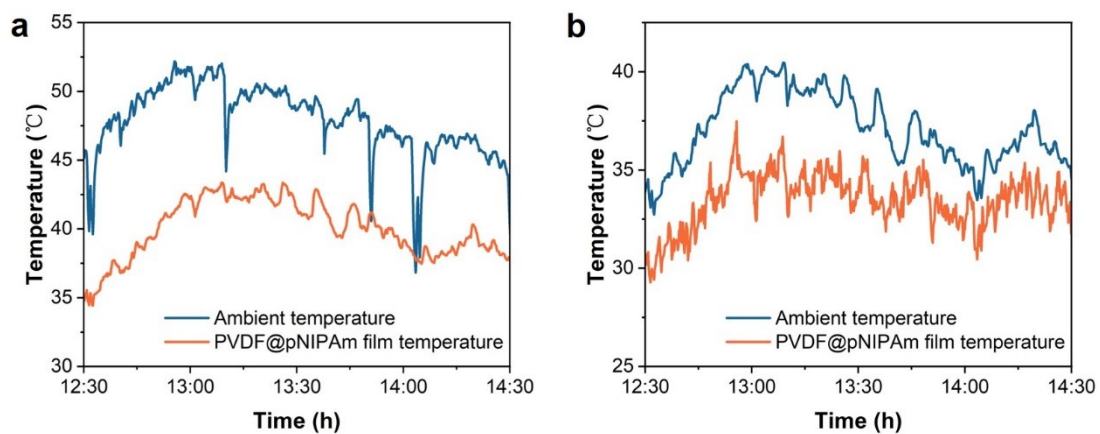


Fig. S11. When covered (a) with LDPE and (b) without LDPE, the recording of the PVDF@pNIPAm film and the ambient temperature under the sunlight at noon. The tests took place on 18 Nov. 2020, and all the environmental conditions remained exactly the same.

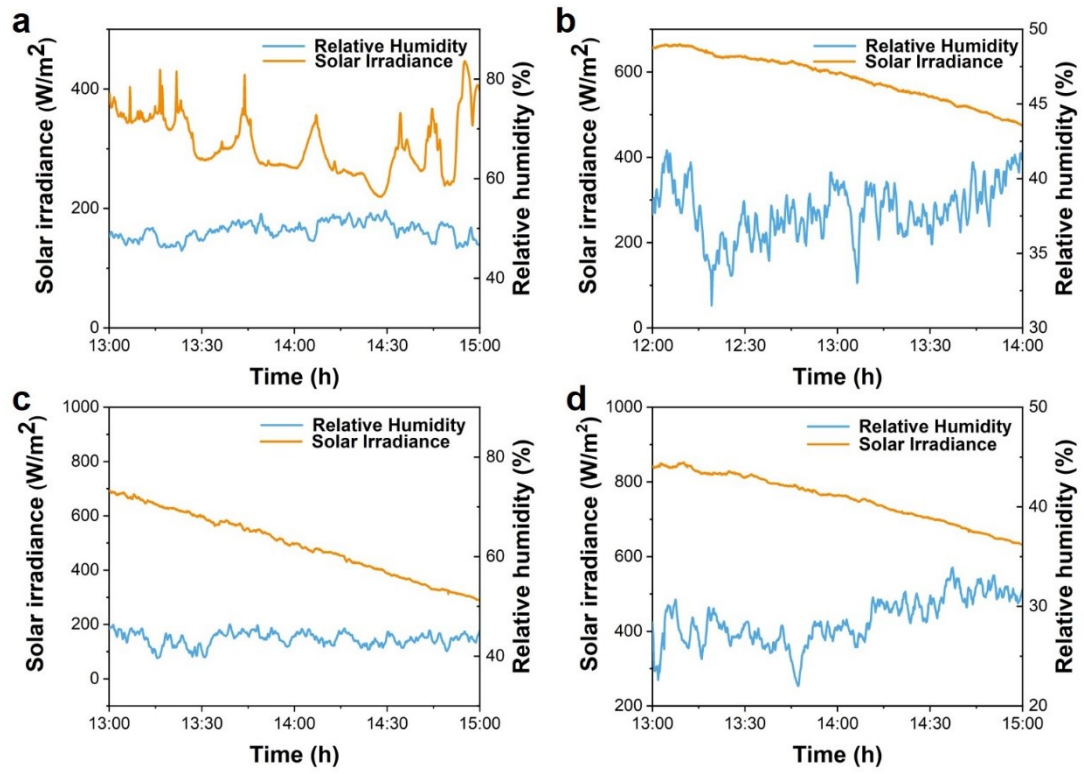


Fig. S12. Solar irradiance and relative humidity in Shanghai on (a) 13 Mar. 2021, (b) 14 Mar. 2021, (c) 18 Nov. 2020, (d) 25 May. 2021.

Table S1. The LCST of pNIPAm hydrogels synthesized with different reactant ratios.

Composition / ratio	1	2	3	4
NIPAm / wt%	7.23	7.14	7.21	10.5
BIS / wt%	0.20	0.20	0.40	0.20
PVA / wt%	1.21	2.38	1.20	1.16
H ₂ O / wt%	91.4	90.3	91.2	88.2
LCST / °C	34	36	33	31

Reference

- 1 M. M. Hossain and M. Gu, *Adv. Sci.*, 2016, **3**, 1500360.
- 2 B. Zhao, M. Hu, X. Ao, N. Chen and G. Pei, *Applied Energy*, 2019, **236**, 489-513.
- 3 T. Wang, Y. Wu, L. Shi, X. Hu, M. Chen and L. Wu, *Nat. Commun.*, 2021, **12**, 365.